OPEN ACCESS

GAVIN PUBLISHERS

Journal of Earth and Environmental Sciences

Salfo K, et al. J Earth Environ Sci 7: 171.

DOI: 10.29011/2577-0640.100171.

Research Article

Solar Cycle Phase and Magnetospheric Convection Electric Filed (MCEF) Time Variation from 1964 to 2009 Under Shock Activity

[1]Kaboré Salfo, [1]Gnabahou Doua Allain, [1,2]Ouattara Frédéric, [2]Zougmoré François

[1]Research Laboratory in Energy and Meteorology of Space (LAREME), University Norbert Zongo (formerly University of Koudougou), Burkina Faso

[2]Labotatory of Materials and Environment (LAME), Ouaga University I Pr Joseph Ki Zerbo, Burkina Faso

***Corresponding author:** Ouattara Frédéric, Research Laboratory in Energy and Meteorology of Space (LAREME), University Norbert Zongo (formerly University of Koudougou, Burkina Faso. Tel: +22676627555; Email: fojals@yahoo.fr

Citation: Salfo K, Allain GD, Frederic O, Francois Z (2019) Solar Cycle Phase and Magnetospheric Convection Electric Filed (MCEF) Time Variation from 1964 to 2009 Under Shock Activity. J Earth Environ Sci 7: 171. DOI: 10.29011/2577-0640.100171.

Received Date: 19 April, 2019; **Accepted Date:** 23 May, 2019; **Published Date:** 03 June, 2019

Abstract

The MCEF time variation is investigated during the geo effectiveness CMEs periods from 1964 to 2009. The shock MCEF time variation shows solar cycle dependence. Through solar cycle phase, the reconnection process begins with northward IMF during solar minimum and decreasing phases. For solar increasing and maximum, the reconnection process starts by southward IMF. During solar maximum phase the IMF remains southward from 0000 UT to 2400 UT. From solar minimum to solar decreasing phase, the shock MCEF mean values are 0.2477 mV/cm, 0.2196 mV/cm, 0.1764 mV/cm and 0.1601 mV/cm, respectively.

Keywords: CMEs; Magnetosphere convection electric field; Solar wind electric field; shock; Solar cycle phases

Introduction

The behaviour of the magnetosphere (created by the solar wind) depends on the solar wind properties and its frozen magnetic field [1]. During the interaction between the solar wind and the planetary magnetosphere we have the following topologies [2], (1) a magnetic line might not intersect the Earth, (2) a magnetic line intersects the Earth with northward z-component and (3) a magnetic line intersects the Earth with southward z-component. During the topologies where a magnetic line intersects the Earth, two mechanisms are invoked to explain such interaction: (a) the mechanism of Axford and Hines [3] [the viscous interaction that is always present] where closed magnetic flux tubes are transported from the dayside to night side, (b) the mechanism of Dungey [4] [magnetism reconnection where the Interplanetary Magnetic Field (IMF) is southward and its field lines convect along by the solar wind break in half and join partners with magnetospheric lines [1].

McPherron et al. [1] notice that the topologies one and two correspond to the geomagnetically quiet time conditions (due to slow solar wind) and the last topology to disturbed conditions (provoked by recurrent and fluctuating solar winds and Coronal Mass Ejections [CMEs]) according to the classification of Legrand and Simon [5]. In fact, these authors, Richardson et al. [6] and Richardson and Cane [7] classified the geomagnetic activity into four classes of activity (quiet, recurrent, fluctuating and shock activities).

For the present study, we considered the disturbed conditions because our objective is to investigate the Magnetosphere Convection Electric Field (MCEF) time variation during the shock activity due to the CMEs. Here we consider the all shock activity. The other types of shock (one-day shock, two-days shock and three-days shock: [8] activity effects will be study later.

By keeping in mind our objective, our investigation is done under the topology where a magnetic line intersects the Earth with southward z-component. For the MCEF investigation we firstly present, the materials and methods used, secondly, the results and discussions and thirdly, conclude.

Materials and Methods

For this paper we investigate the all shock MCEF [8] and Kaboré and Ouattara [9] for more details] diurnal variation for different solar cycle phases. The solar cycle phases are determined

by means of the sunspot number (Rz). To determine the geomagnetic activity, we use the Mayaud [10,11] geomagnetic index aa and the sudden storm commencement (SSC) dates. The MCEF values are carried out by means of the values of the Solar Wind Electric Field (SWEF) y-component (Ey)

The method for determining the solar cycle phases

For the determination of the years of the four solar cycles, we use the sunspot number Rz under the following criteria [8,12-15]: (1) minimum phase: Rz < 20; (2) ascending phase : 20 ≤ Rz ≤ 100 and Rz greater than the previous year's value; (3) maximum phase : Rz >100 [for small solar cycles (solar cycles with sunspot number maximum (Rz max) less than 100) the maximum phase is obtained by considering Rz > 0.8*Rz max]; and (4) descending phase: 100 ≥ Rz ≥ 20 and Rz less than the previous year's value. In these previous inequations, Rz is the yearly average Zürich sunspot number.

The method for determining the shock activity

We use the pixel diagrams (Figure 1) that show the repartition of the geomagnetic data as a function of the solar activity as described by solar rotation (27 days) [8,16]. It can be seen in these diagrams the four classes of geomagnetic activity [5] as highlighted in the (Figure 1).

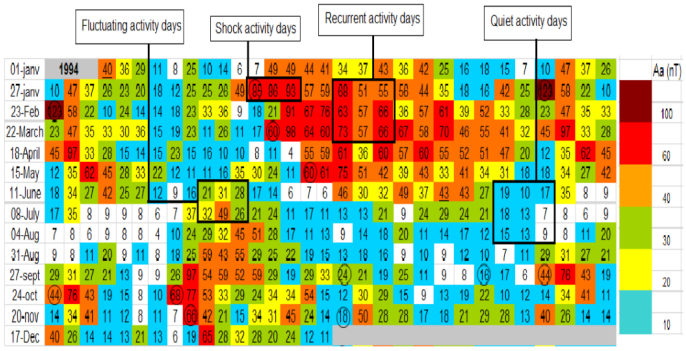

Figure 1: The four geomagnetic activities [16].

The method for determining the magnetospheric convection electric field

For MCEF (E_M) hourly values determination, we follow the method of Kaboré and Ouattara [9]. This method consists of using the linear correlation between the hourly data of the SWEF (E_y) and that of the MCEF established by [17]. This equation is : $E_M = 0.13\ E_y + 0.09$ with the correlation coefficient (r) value of 0.97. The hourly values of the MCEF are computed through the above equation and for the period 1964-2009 while those of the SWEF can be find in OMNIWEB web site : *http://omniweb.gsfc.nasa.gov/form/dx1.html*

Results and Discussions

(Figure 2) shows the daytime variability of the shock MCEF during the solar cycle minimum phase. One can see that the shock MCEF graph shows a decreasing phase from 0000 UI to 0900 UT and an increasing phase from 0900 UT to 24000 UT. The decreasing trend slop is $-\frac{2.15\,10^{-2}mV}{cm.s}$ with correlation coefficient 0.8461 and that of the increasing trend is $+\frac{1.16\,10^{-2}mV}{cm.s}$ with correlation coefficient value 0.7188.

During the minimum phase, between 0000 UT and 0900 UT, the shock MCEF values vary from 0.3079 mV/cm to 0.0876 mV/cm with 0.2094 mV/cm as its mean value while between 0900 UT and 2400 UT the shock MCEF values vary from 0.0876 mV/cm to 0.3783 mV/cm with a mean value of 0.2732 mV/cm. Finally, the shock MCEF mean value from 0000 UT to 2400 UT is 0.2477 mV/cm.

The two trends exhibited by solar cycle minimum phase graph present the same behaviour as that of quiet time period [9] but each trend time interval is shorter than that of quiet time.

To interpret the two trends of the shock MCEF, we can convoke the model of Axford and Hines [3] which let us assert that there is the lack of closed magnetic flux tubes (decreasing phase) and the accumulation of the flux tubes (increasing phase) by viscous interaction. The using of Dungey [4] model let also assert that the impact of the shock activity starts at 0900 UT. In fact, the decreasing trend period (0000 UT-0900 UT) maybe characterized the period where act the northward Interplanetary Magnetic Field (IMF). This topology remains until 0900 UT where the IMF turns southward. At that time the reconnection occurs and the MCEF increases.

This interpretation is also expressed by Nishimura et al. [18] who noted that the MCEF reacts to this change and de Siqueira et al. [19] who underline that the MCEF increases after the change of the IMF from northward to southward. This explanation is also sustained by Partamies et al. [20]. For them, the period of the increasing phase of the MCEF corresponds to the sustained southward IMF and consequently shows the storm main phase. The beginning of this phase corresponds to the onset time of the change of the IMF from northward to southward. According to Kaboré and Ouattara [9] the increasing phase of the MCEF expressed the phase where geomagnetic activity increases.

The decreasing phase which occurs after the increasing phase shows the phase of the change of the IMF from southward to northward. In fact, according to Kelley et al. [21] the magnetospheric convection is weakened when the IMF turns from southward to northward. The following increasing phase may be due to the change of the IMF from northward to southward.

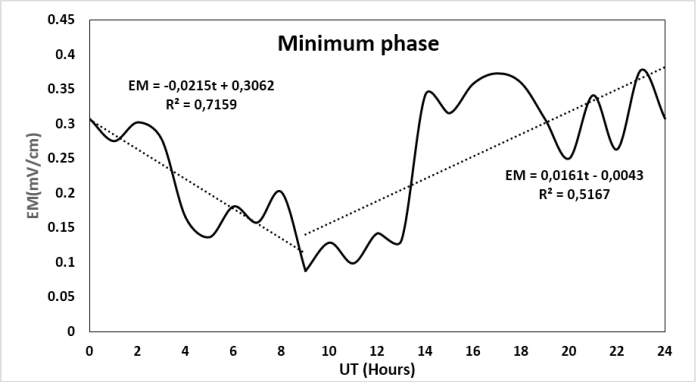

Figure 2: All shock magnetosphere convection electric field time variation during solar minimum phase.

The (Figure 3) shows the time variation of the shock MCEF during the solar increasing phase. We have three trends. The increasing trend from 0000 UT to 0900 UT with the slope of $+\frac{2.06\,10^{-2}mV}{cm.s}$ and the correlation coefficient of 0.9173 follows by the decreasing one from 0900 UT to 1800 UT with the slope of $-\frac{3.32\,10^{-2}mV}{cm.s}$ and the correlation coefficient of 0.9626. The last trend is and increasing one from 1800 UT to 2400 UT with the slope of $+\frac{1.38\,10^{-2}mV}{cm.s}$ and the correlation coefficient of 0.6324.

It can be noted that the graph behaviour looks like that of the shock for the whole solar cycle (see [9]) with a shorter trend time interval.

During the increasing phase, between 0000UT and 0900 UT, the shock MCEF values vary from 0.1858 mV/cm to 0.3531 mV/cm with 0.2855 mV/cm as its mean value while between 0900 UT and 1800 UT the shock MCEF values vary from 0.3531mV/cm to 0.0741 mV/cm with a mean value of 0.1963 mV/cm and between 1800 UT and 2400 UT the shock MCEF values vary from 0.0741 mV/cm to 0.1858 mV/cm with 0.1571 mV/cm as its mean value.

These situation leads to 0.2196 mV/cm as the shock MCEF during the increasing phase.

The period of the increasing phase of the shock MCEF corresponds to the sustained southward IMF and consequently shows the storm main phase. The beginning of this phase corresponds to the onset time of the change of the IMF from northward to southward. The following trend is a decreasing one that trend change shows a new reconnection with northward IMF. After this new reconnection, the IMF remains northward until 1800 UT and at that time turns again southward. This situation is expressed by the increasing trend from 1800 UT to 2400 UT.

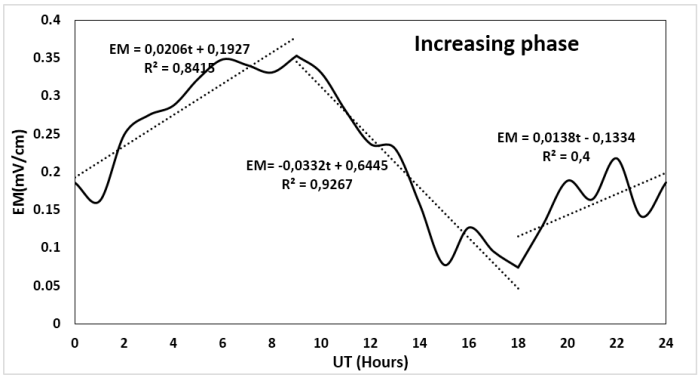

Figure 3: The same as figure 2 but for the increasing phase.

The (Figure 4) is devoted to the time variation of the shock MCEF for the maximum phase. The shock MCEF increases from 0000 LT to 2400 LT with the slop value of $+\frac{2.2\,10^{-3}mV}{cm.s}$ and 0.6373 as the correlation coefficient value. The shock MCEF oscillates between its minimum value (0.1204 mV/cm) and its maximum value (0.2434 mV/cm) with a mean value of 0.1764 mV/cm. This one trend is characteristic. It expresses that the IMF at all time is southward at solar maximum phase. But when we carefully observed the shock MCEF graph, it can be observed an eight successive change of direction of the IMF from North to South.

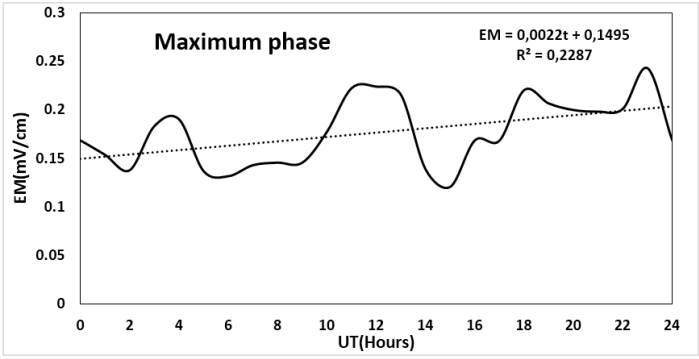

Figure 4: The same as (Figure 2) but for the maximum solar cycle phase.

The (Figure 5) concerns the shock MCEF time variation during solar cycle decreasing phase.

During this solar cycle phase, the shock MCEF exhibits two trends. The first one is a decreasing trend and is the longest. It begins at 0000 UT and ends at 2100 UT. This trend corresponds to the reconnection with a northward IMF. The trend slope is $-\frac{4.7\,10^{-3}mV}{cm.s}$ with the correlation coefficient of 0.6382. The shock MCEF oscillates between its minimum value (0.0774 mV/cm) and its maximum value (0.2381 mV/cm) with a mean value of 0.1601

mV/cm. This one trend is characteristic. The second trend is an increasing one which begins at 2100 UT and finishes at 2400 UT.

The slope of this trend is $+\frac{4.54\,10^{-2}mV}{cm.s}$) with a correlation coefficient of 0.9627. This positive trend highlights the reconnection with a southward IMF.

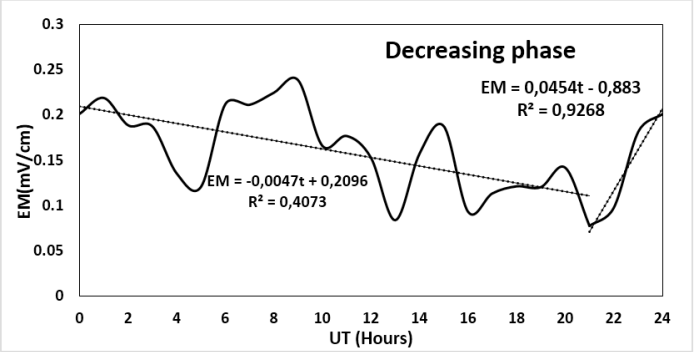

Figure 5: The same as figure 2 but for the decreasing solar cycle phase.

Conclusion

The present work shows that the mean amplitudes of the shock MCEF are higher during the minimum and the decreasing solar cycle phases than that of the maximum and the increasing phase. For the first ones we have 0.2477 mV/cm and 0.2196 mV/cm, respectively and for the last ones we have 0.1764 mV/cm and 0.1601 mV/cm, respectively.

The shock MCEF graph trends exhibit solar cycle phase dependence. In fact, through solar cycle phase, the shock MCEF presents (1) two different trends (decreasing follows by the increasing one) for the minimum and the decreasing phases, (2) three trends (increasing, decreasing and increasing) during the increasing phase and (3) one trend (increasing) for the maximum phase.

During the minimum phase, between 0000 UT and 0900 UT, the shock MCEF values vary from 0.3079 mV/cm to 0.0876 mV/cm while between 0900 UT and 2400 UT the shock MCEF values vary from 0.0876 mV/cm to 0.3783 mV/cm. At the increasing phase, between 0000UT and 0900 UT, the shock MCEF values vary from 0.1858 mV/cm to 0.3531 mV/cm while between 0900 UT and 1800 UT the shock MCEF values vary from 0.3531mV/cm to 0.0741 mV/cm. Between 1800 UT and 2400 UT the shock MCEF values vary from 0.0741 mV/cm to 0.1858 mV/cm. For solar maximum, the shock MCEF oscillates between its minimum value (0.1204 mV/cm) and its maximum value (0.2434 mV/cm). At solar decreasing phase the shock MCEF oscillates between its minimum value (0.0774 mV/cm) and its maximum value (0.2381 mV/cm).

Acknowledgment

The authors thank the all data providers.

References

1. RL McPherron, JM Weygand, TS Hsu (2007) J Solar Terr Phys.
2. CT Russel (1979) University of Alaska, Geophysical Institute, Elvey CT Building, Fairbanks, Alaska, USA 3-21.
3. WI Axford, CO Hines (1961) A Unifying Theory of High-Latitude Geophysical Phenomena and Geomagnetic Storms. Canadian Journal of Physics 39: 1433-1464.
4. JW Dungey (1961) Interplanetary magnetic field and the auroral zones. Phys Rev Lett 6: 47-48.
5. JP Legrand, PA Simon (1989) Annals of Geophysics 7: 565-578.
6. IG Richardson, EW Cliver, HV Cane (2000) Journal of Geophysical Research 105: 18200-18213.
7. IG Richardson, HV Cane (2002) Sources of geomagnetic activity during nearly three solar cycles (1972–2000). Journal of Geophysical Research 107: 1187.
8. AMF Gyébré, DA Gnabahou, F Ouattara (2018) The Geomagnetic Effects of Solar Activity as Measured at Ouagadougou Station. International Journal of Astronomy and Astrophysics 8: 178-190.
9. S Kaboré, F Ouattara (2018) Magnetosphere convection electric field (MCEF) time variation from 1964 to 2009: Investigation on the signatures of the geoeffectiveness coronal mass ejections. Int J Phys Sci 13: 273-281.
10. PN Mayaud (1971) Annales Geophysicae 27: 67-71.
11. PN. Mayaud (1972) The aa indices: A 100□year series characterizing the magnetic activity. Journal of Geophysical Research 77: 6870-6874.
12. JL Zerbo, F Ouattara, C Zoundi, AMF Gyébré (2011) Revue CAMES-Série A 12: 255-262.
13. F Ouattara F, MN Ali, F Zougmoré, Eur (2012) Sci J 1-14.
14. A Gnabahou, F Ouattara (2012) Ionosphere Variability from 1957 to 1981 at Djibouti Station. European Journal of Scientific Research 73: 382-390.
15. F Ouattara (2013) Scholars Research Library Archives of Physics Research 4:12-18.
16. F Ouattara, C Amory Mazaudier, J Atmos (2009) Solar-Terr Phys 71:1736-1748.
17. I Revah, P Bauer (1982) Note technique, CRPE/115, 3840, Rue du Général Leclerc, 92131, Issy-les moulineaux 108.
18. Y Nishimura, T Kikuchi, J Wygant, A Shinbori, T Ono (2009) J Geophys Res 114: 1-11.
19. PM Siqueira, ER Paula, MTAH Muella, LFC Rezende, MA Abdu (2011) Ann Geophys 29: 1765-17778.
20. N Partamies, I Juusola, E Tanskanen, K Kauristie, JM Weygand, et al. (2011) Ann Geophys 29 : 2011-2043.

21. MC Kelly, BG Fejer, CA Gonzales (1979) Geophys Res Let 6, 301-304.

22. T Gold (1959) J Geophys Res 64: 1219-1224.

23. WD Gonzalez, JA Joselyn, Y Kamide, HW Kroehl, G Rostoker, et al. (1994) What is a geomagnetic storm?. J Geophys Res 99: 5771-5792.

24. AMF Gyébré, F Ouattara, S Kaboré, JL Zerbo (2015) British Journal of Science 13 (1) 1-7.

25. J Lilensten, PL Blelly (2000) Du soleil à la Terre : Aéronomie et Météorologie de l'Espace. Presses Universitaires de Grenoble, Grenoble.

26. AJ Mannucci, BT Tsurutani, MA Abdu, WD Gonzalez, A Komjathy, et al. (2008) Superposed epoch analysis of the dayside ionospheric response to four intense geomagnetic storms. J Geophys Res 113.

27. F Ouattara, S Kaboré, AMF Gyébré, JL Zerbo (2015) Time Variation of Shock Activity due to Moderate and Severe CMEs from 1966 to 1998. European Journal of Scientific Research 153-159.

28. F Ouattara, DA Gnabahou, C Amory-Mazaudier (2012) Seasonal, Diurnal, and Solar-Cycle Variations of Electron Density at Two West Africa Equatorial Ionization Anomaly Stations. International Journal of Geophysics 9.

29. F Ouattara (2009) PhD thesis, Contribution à l'étude des relations entre les deux composantes du champ magnétique solaire et l'ionosphère équatoriale, Université Cheikh Anta Diop de Dakar, (Dakar, SENEGAL).

30. CT Russel, Volker Bothmer, Loannis A (2007) Space weather - Physics and effects. Daglis (ed.) Springer, Praxis Publishing, Chichester UK 103-130.

31. A Tommaso, P Mirko, V Antonio, DM Paula, L Fabio, et al. (2016) Ann. Geophys 34: 1069-1084.